

EUROPEAN LABORATORY FOR PARTICLE PHYSICS

CERN - LHC DIVISION

---

LHC-VAC/OBM/mpt

Vacuum Technical Note 99-05  
April 1999

**The effect of the temperature  
and of a thick layer of condensed CO<sub>2</sub> on the photoelectron  
emission and on the photon reflection**

*V.V. Anashin, A.A. Krasnov, O.B. Malyshev and E.E. Pyata*

## 1. Introduction

Most of the length of the LHC vacuum chamber will be at cryogenic temperature. The high intensity photon flux will stimulate photoelectron emission from the wall of the LHC vacuum chamber. The photoelectrons can participate in the different processes in the vacuum chamber, the more important ones are the gas photodesorption and the beam induced multipactoring. The aim of the present work was to study the important question: How much a layer of condensed gas may change the photoelectron emission with the photons irradiating the vacuum chamber at grazing incidence?

This note describes the study performed between March to May 1998 within the frame of the collaboration between CERN and the Budker Institute of Nuclear Physics, Novosibirsk, Russia (see item 1.5). [1].

## 2. Set-up

The existing ‘close geometry’ set-up which was previously used to measure the photodesorption of cryosorbed gases [2] was modified to measure the photocurrent from the substrate with the condensed gas layer under the synchrotron radiation. The layout of the central part of the installation is shown in Fig. 1. The test tube was made of a 1m long stainless steel tube (ID=32 mm) with electro-deposited Cu. The temperature of the test tube could be either room temperature or the temperature of the corresponding liquid in the cryostat. An electrically-isolated collector was installed coaxially at the end of the chimney as an additional measuring instrumentation. This is a disk with an area  $A_{\text{col}} = 0.75 \text{ cm}^2$  which remains at room temperature irrespective of the temperature of the test tube. The potential of the collector can be varied in the range  $\pm 300 \text{ V}$ . The current from the collector was measured with a low current transducer. The low limit of the current measurement is  $10^{-14} \text{ A}$  at zero potential and  $10^{-11} \text{ A}$  at  $+300 \text{ V}$ .

In experiments with condensed gas, the experimental volume was filled with CO<sub>2</sub>, measured by the absolute pressure transducer (BARATRON) and cooled to about 69 K. During irradiation, the gas density was measured by the residual gas analyser (RGA).

In all experiments the grazing photon incident angle was about 10 mrad. The electrode is opposite to the directly irradiated surface.

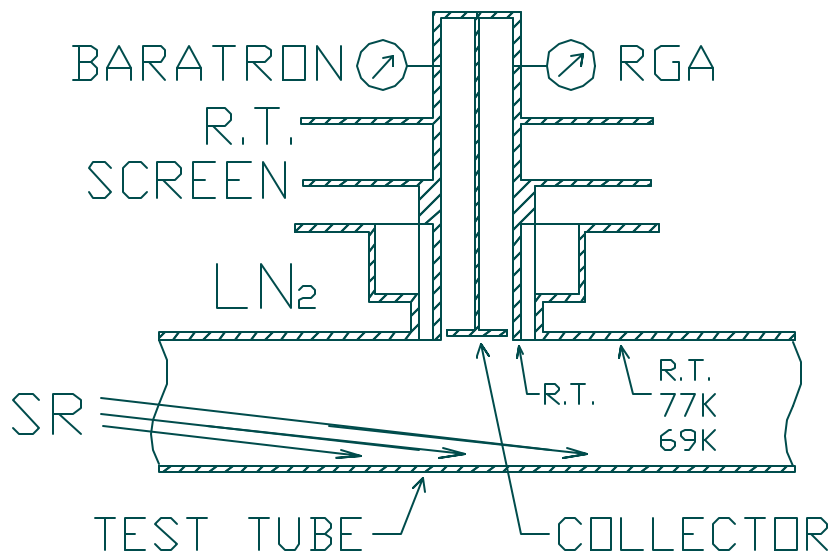


**Figure 1. The experimental layout**

### 3. Experiment

In all experiments both the photoelectron current and the gas pressure were measured. The results are presented as a photoelectron current measured from collector,  $I_{col}$ , corresponding to the photon flux  $\dot{\Gamma} = 10^{16}$  photon/(sec·m).

The photoelectron yield was studied as a function of the condensed gas surface coverage at different bias potential on the electrode-collector.

### **The runs of the experiment**

1. The measurements at room temperature with a bare surface.
2. The measurements at  $T \approx 77$  K with a bare surface.
3. The measurements at  $T \approx 68$  K with about 1000 monolayers of condensed  $\text{CO}_2$ .
4. The measurements at room temperature with bare surface.
5. The measurements at  $T \approx 68$  K with about 100 monolayers of condensed  $\text{CO}_2$ .

The results of the measurements with the collector are presented in Fig. 2.

The collector potential was varied in the range from  $-300$  V to  $+300$  V. At negative potential only photoelectrons emitted due to reflected photons reaching the collector are observed. The saturated value is reached at about  $-10$  V for all experiments. At positive potential, the photoelectrons from vacuum chamber wall are collected on the electrode-collector. The measured current increases with the potential but does not become saturated even at the highest potential of  $+300$  V. This effect is attributed to the fact that with a higher potential, the photoelectrons from a longer part of the vacuum chamber are collected.

The ratio of the photocurrents in different experiments to the photocurrent in the vacuum chamber at room temperature is shown in Table 1. The photoelectron yield from the collector at negative potential decreases with coverage of cryosorbed  $\text{CO}_2$ . Since only diffusely reflected photons can irradiate the collector, one could conclude that the flux of diffusely reflected photons from the surface with condensed gas is reduced. The photoelectron current of the collector for positive potential also decreases with the coverage of cryosorbed  $\text{CO}_2$ , but the ratio  $I_{\text{col}}/I_{\text{col}}(300\text{K})$  for positive potential is smaller than for a negative bias, hence the photoelectron yield from the surface with condensed gas is reduced.

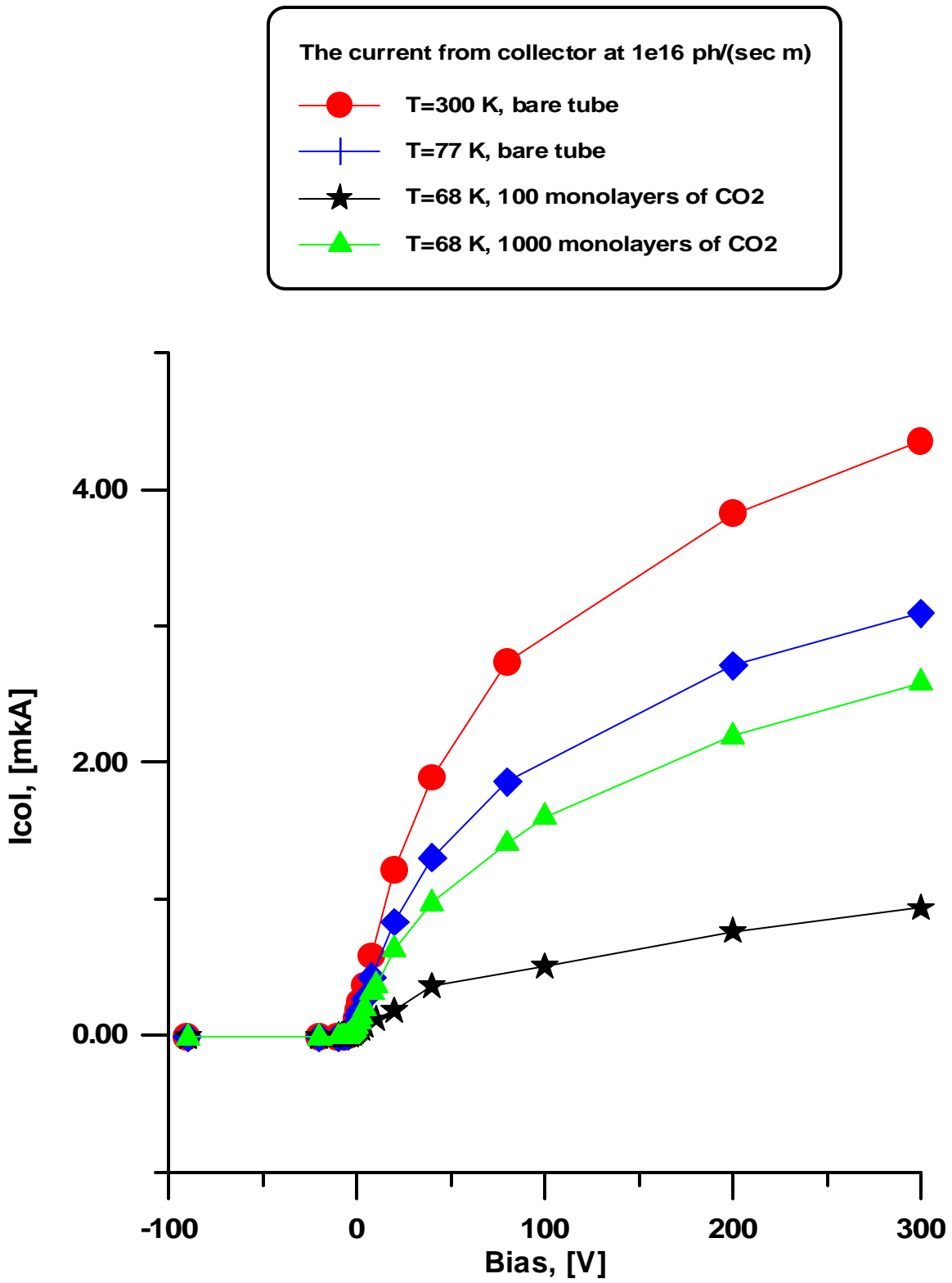


Figure 2. The measured current from collector as a function of bias

**Table 1**

The ratio of photocurrent in experiments to the photocurrent in Run 1 at T=300 K

	I <sub>col</sub> /I <sub>col</sub> (300K)		
	U = - 10 V	U = 0 V	U = + 300 V
The bare tube at T=77 K	0.87	0.84	0.74
T≈69 K, 100 monolayers of CO <sub>2</sub>	0.91	0.6	0.63
T≈69 K, 1000 monolayers of CO <sub>2</sub>	0.45	0.25	0.23

As an additional result, Table 3 shows the residual gas spectrum in the test vacuum chamber with and without irradiation. The lines with 'Δ' show the pressure rise due to photo-stimulated desorption. The vacuum chamber was stored at high vacuum before beginning these measurements; this is the reason why the gas density without photons is much less in Run 1 and Run 2 compared to Run 4. The latter was done following a short warm-up after Run 3, and showed that a large quantity of gas remains on the walls of the vacuum chamber and on the RGA tube.

It is interesting to compare the spectrum in Run 3 and Run 5. The pressure rise of CO is about 4–5 times higher than for CO<sub>2</sub>, the pressure rise of O<sub>2</sub> is about 15–20 times higher than for CO<sub>2</sub>. That again confirms the effect of cracking of condensed molecules of CO<sub>2</sub> into CO and O<sub>2</sub> molecules [3,4,5] via the process:  $2CO_2 + \tilde{g} \rightarrow 2CO + O_2$ .

The gas density can be described as [6]:

$$n_i = \frac{(\mathbf{h}_i + \mathbf{h}'_i(s_i) + \mathbf{c}_i(s_j))\dot{\Gamma}}{\mathbf{s}_i S_i} + n_e(s_i);$$

where the index  $i$  denotes the gas species in the residual gas spectrum;

$n$  [molecules/cm<sup>3</sup>] is the volume molecular density;

$s$  [molecules/cm<sup>2</sup>] is the surface molecular density;

$\dot{\Gamma}$  [photon/sec] is the photon intensity;

$h$  [molecules/photon] is the primary photodesorption yield;

$h'$  [molecules/photon] is the photodesorption yield of crysorbed molecules (secondary photodesorption yield);

$s$  is the sticking probability;

$c_i(s_j)$  [molecules/photon] is the cracking yield which determines how many type  $i$  molecules are created due to cracking of type  $j$  molecules per photon.

$S_i = A\bar{v}_i/4$  [cm<sup>3</sup>/sec] is the ideal wall pumping speed,  $\bar{v}_i$  is mean molecular speed for the gas  $i$ ;

$n_e$  [molecules/cm<sup>3</sup>] is the thermal equilibrium gas density.

In this experiment, the primary desorption and the equilibrium gas density can be neglected, hence it is possible to estimate the values of the cracking yield and of the secondary desorption from the layer of CO<sub>2</sub> by using the following expressions:

$$n_{CO_2} = \frac{(h_i + h'_i(s_{CO_2}) + c_i(s_{CO_2}))\dot{\Gamma}}{s_{CO_2}S_{CO_2}};$$
$$n_{O_2} = \frac{c_{O_2}(s_{CO_2})\dot{\Gamma}}{s_{O_2}S_{O_2}};$$
$$n_{CO} = \frac{c_{CO}(s_{CO_2})\dot{\Gamma}}{s_{CO}S_{CO}}.$$

The measured value is the room temperature partial pressure,  $P_i = n_i k_B \sqrt{T_{RT} \cdot T_{cryo}}$ , here  $k_B$  is the Boltzman constant,  $T_{RT}$  is a room temperature (the RGA's temperature) and  $T_{cryo}$  is the temperature of test vacuum chamber. Hence:

$$\frac{h'_{CO_2}}{s_{CO_2}} = \frac{P_{CO_2} S_{CO_2}}{\dot{\Gamma} k_B \sqrt{300 \cdot 68}};$$

$$\frac{c_{O_2}}{s_{O_2}} = \frac{P_{O_2} S_{O_2}}{\dot{\Gamma} k_B \sqrt{300 \cdot 68}};$$

$$\frac{c_{CO}}{s_{CO}} = \frac{P_{CO} S_{CO}}{\dot{\Gamma} k_B \sqrt{300 \cdot 68}}.$$

The estimates with these formulae are presented in Table 2.

**Table 2**

The secondary desorption of CO<sub>2</sub> and cracking yields of CO and O<sub>2</sub> from the layer of condensed CO<sub>2</sub>

	$\frac{c_{CO}}{s_{CO}}$	$\frac{c_{O_2}}{s_{O_2}}$	$\frac{h'_{CO_2}}{s_{CO_2}}$
Run 3	$6 \cdot 10^{-2}$	0.24	$1.1 \cdot 10^{-2}$
Run5	$6 \cdot 10^{-2}$	0.12	$6.4 \cdot 10^{-3}$

The sticking probability for CO<sub>2</sub> is close to unity for high coverages between 100–1000 monolayers. From the formula  $2CO_2 + \tilde{g} \rightarrow 2CO + O_2$  one may expect:  $c_{CO}/c_{O_2} = 2$ . Unfortunately, there are no data available on the sticking probability for O<sub>2</sub> and for CO on a condensed layer of CO<sub>2</sub> at T = 68 K. Therefore, the relatively large value  $c_{O_2}/s_{O_2}$  can be explained only when the sticking probability for O<sub>2</sub> is much less than for CO.

Another interesting effect is that the H<sub>2</sub> pressure decreases in the presence of photons in experiments 3 and 5, see negatives  $\Delta$  values in Table 3. The cryo-trapping of H<sub>2</sub> molecules with CO, O<sub>2</sub> and CO<sub>2</sub> looks a good (quite real) explanation of this effect.

**Table 3**

The partial pressure of different gases in experiment

Run	T, [K]	s(CO <sub>2</sub> ) [mono-layers]	$\dot{\Gamma}$ , [ $\frac{\text{phot}}{\text{sec}\cdot\text{m}}$ ]	P <sub>H<sub>2</sub></sub> (M=2) [Torr]	P <sub>H<sub>2</sub>O</sub> (M=18) [Torr]	P <sub>CO</sub> (M=28) [Torr]	P <sub>O<sub>2</sub></sub> (M=32) [Torr]	P <sub>CO<sub>2</sub></sub> (M=44) [Torr]
1	300	0	0	$6\cdot 10^{-9}$	$2\cdot 10^{-9}$	$0.7\cdot 10^{-8}$	$10^{-11}$	$7\cdot 10^{-10}$
			$10^{16}$	$5\cdot 10^{-8}$	$3.4\cdot 10^{-8}$	$1.9\cdot 10^{-8}$	$10^{-11}$	$4.3\cdot 10^{-7}$
			$\Delta$	<b><math>4.4\cdot 10^{-8}</math></b>	<b><math>3.2\cdot 10^{-8}</math></b>	<b><math>1.2\cdot 10^{-8}</math></b>	<b>0</b>	<b><math>3.7\cdot 10^{-7}</math></b>
2	77	0	0	$5\cdot 10^{-9}$	$8\cdot 10^{-10}$	$1.5\cdot 10^{-8}$	$10^{-11}$	$1.3\cdot 10^{-10}$
			$10^{16}$	$1.7\cdot 10^{-8}$	$8\cdot 10^{-10}$	$1.7\cdot 10^{-8}$	$10^{-11}$	$3.8\cdot 10^{-10}$
			$\Delta$	<b><math>1.2\cdot 10^{-8}</math></b>	<b>0</b>	<b><math>2\cdot 10^{-9}</math></b>	<b>0</b>	$2.5\cdot 10^{-10}$
3	68	1000	0	$5.9\cdot 10^{-8}$	$1.5\cdot 10^{-8}$	$10^{-8}$	$10^{-10}$	$10^{-8}$
			$10^{16}$	$1.4\cdot 10^{-8}$	$2.5\cdot 10^{-8}$	$1.6\cdot 10^{-7}$	$6.5\cdot 10^{-7}$	$4.3\cdot 10^{-8}$
			$\Delta$	<b><math>-4.5\cdot 10^{-8}</math></b>	<b><math>1\cdot 10^{-8}</math></b>	<b><math>1.5\cdot 10^{-7}</math></b>	<b><math>6.5\cdot 10^{-7}</math></b>	<b><math>3.3\cdot 10^{-8}</math></b>
4	300	0	0	$10^{-7}$	$2.6\cdot 10^{-7}$	$8\cdot 10^{-9}$	$10^{-10}$	$4.6\cdot 10^{-9}$
			$10^{16}$	$10^{-7}$	$2.3\cdot 10^{-7}$	$3.2\cdot 10^{-8}$	$10^{-10}$	$2.7\cdot 10^{-8}$
			$\Delta$	<b>0</b>	<b><math>3\cdot 10^{-8}</math></b>	<b><math>2.4\cdot 10^{-8}</math></b>	<b>0</b>	<b><math>2.2\cdot 10^{-8}</math></b>
5	68	100	0	$10^{-7}$	$1.4\cdot 10^{-8}$	$10^{-8}$	$10^{-10}$	$5.4\cdot 10^{-9}$
			$10^{16}$	$10^{-8}$	$1.4\cdot 10^{-8}$	$1.6\cdot 10^{-7}$	$3.3\cdot 10^{-7}$	$2.6\cdot 10^{-8}$
			$\Delta$	<b><math>-9\cdot 10^{-8}</math></b>	<b>0</b>	<b><math>1.5\cdot 10^{-7}</math></b>	<b><math>3.3\cdot 10^{-7}</math></b>	<b><math>2.0\cdot 10^{-8}</math></b>

## 4. Conclusion

1. The diffuse photon reflectivity decreases with the amount of cryosorbed CO<sub>2</sub>.

2. The photoelectron yield decreases with the amount of cryosorbed CO<sub>2</sub>.
3. The gas density measurements confirm the effect of cracking for cryosorbed CO<sub>2</sub> into CO and O<sub>2</sub>.
4. The gas density measurements show the cryo-trapping effect for H<sub>2</sub> in presence of synchrotron radiation.

## References

1. Addendum No. A3 to the Protocol dated 14 June 1996 to the 1993 Cooperation Agreement between CERN and the Government of the Russian Federation concerning the Russian participation in the Large Hadron Collider project (LHC). CERN-BINP, 1997.
2. V.V. Anashin, O.B. Malyshev, R. Calder, O. Gröbner and A.G. Mathewson. Photon induced molecular desorption from condensed gases. *Vacuum* v.48, No. 7–9, 1997, pp. 785–788.
3. V.V. Anashin, O.B. Malyshev, R. Calder, O. Gröbner and A.G. Mathewson. The study of photodesorption processes for cryosorbed CO<sub>2</sub>. *Nuclear Instruments & Methods in Physics Research A* 405, 1998, pp. 258–261.
4. V.V. Anashin, O.B. Malyshev, R. Calder, O. Gröbner. A study of the photodesorption process for cryosorbed layers H<sub>2</sub>, CH<sub>4</sub>, CO and CO<sub>2</sub> cryosorbed between 3 K and 68 K, *Vacuum* 53 (1999), pp. 269-272.
5. V. Baglin. Etude de la photo-désorption de surfaces techniques aux températures cryogéniques. Doctorat thèse. Université Denis Diderot Paris & UFR de Physique, Paris, Mai 1997.
6. O.B. Malyshev, V.V. Anashin, I.R. Collins and O. Gröbner. Photodesorption processes including cracking of molecules in a cryogenic vacuum chamber, to be published as LHC Project Report.